

JCTC

Journal of Chemical Theory and Computation

New Formulation and Implementation of Vibrational Self-Consistent Field Theory

Mikkel B. Hansen,^{*,†} Manuel Sparta,[†] Peter Seidler,[†] Daniele Toffoli,^{‡,‡} and Ove Christiansen[†]

The Lundbeck Foundation Center for Theoretical Chemistry, Center for Oxygen Microscopy and Imaging, Department of Chemistry, University of Aarhus, Langelandsgade 140, DK 8000 Aarhus C, Denmark, and Department of Chemistry, Middle East Technical University, 06531 Ankara, Turkey

Received August 20, 2009

Abstract: A new implementation of the vibrational self-consistent field (VSCF) method is presented on the basis of a second quantization formulation. A so-called active terms algorithm is shown to be a significant improvement over a standard implementation reducing the computational effort by one order in the number of degrees of freedom. Various types of screening provide even further reductions in computational scaling and absolute CPU time. VSCF calculations on large polyaromatic hydrocarbon model systems are presented. Further, it is demonstrated that in cases where distant modes are not directly coupled in the Hamiltonian, down to linear scaling of the required CPU time with respect to the number of vibrational modes can be obtained. This is illustrated with calculations on simple model systems with up to 1 million degrees of freedom.

1. Introduction

A central topic in modern theoretical chemistry is the search for linear scaling algorithms for the calculation of the electronic structure of molecular systems. By linear scaling it is meant that the computational effort scales linearly with the size of the system. While traditionally electronic structure methods have had much steeper computational scaling, there has been significant progress in reducing the computational scaling, in particular with respect to the self-consistent field types of methods including Hartree–Fock and density functional theory.^{1–3} While linear scaling methods for more advanced and accurate electronic structure methods have been more slow in coming, there have been activity and progress along these lines as well.^{3–6}

While calculation of the electronic structure is a very fundamental issue and in many cases the logical first step toward a theoretical description of a molecule, understanding the dynamics of large and complex systems is another fundamental challenge of modern theoretical chemistry. In

that framework the working conditions have been significantly different. Classical molecular dynamics (MD) is probably still the most widely used tool for studying the dynamics of large molecular systems. However, classical MD per definition involves a fundamental error in the complete neglect of quantum effects. On the other hand, quantum dynamical methods have generally proven to have a very steep, often exponential, computational scaling with the size of the system. Thus, quantum dynamical methods have very rarely been applicable to larger systems.^{7–9} Obviously, this is a problem as more and more research, both theoretical and experimental, focuses on large molecular systems.

The self-consistent field method in either time-independent form, known as vibrational self-consistent field (VSCF) theory,^{10,11} or in the time-dependent form (TD-SCF), sometimes also denoted time-dependent Hartree (TDH), is complementary to classical MD in two ways: (i) the theory is completely quantum mechanical in nature in contrast to the classical MD; (ii) it involves the construction of the best possible separation of motion in a self-consistently determined mean field in contrast to the full correlation of the degrees of freedom in classical MD. In this study we shall discuss further the use of VSCF. As in electronic Hartree–

* Corresponding author e-mail: mbh@chem.au.dk.

[†] University of Aarhus.

[‡] Middle East Technical University.

Fock theory, the VSCF method from the outset involves significant approximations. However, VSCF is sometimes good enough, and furthermore it acts as the stepping stone to a variety of more advanced approaches.

It has very recently been shown that for a Hamiltonian coupling at most two modes, advanced methods such as vibrational coupled cluster (VCC) with up to two-mode excitations (VCC[2]) can be made to scale cubically with the system size.¹² In the limit where each mode has only significant interactions with a limited set of other modes, essentially linear scaling was demonstrated for the key steps in the VCC algorithm. However, the relevance of this is based on the assumption that the VSCF state can be obtained in an insignificant amount of time, since usually VSCF provides the reference state and optimal one-mode basis functions. In this paper, we illustrate how VSCF in a simple implementation also scales cubically for a two-mode Hamiltonian, but a much improved active terms algorithm can bring down the scaling to quadratic. Introducing various screenings and other tricks, the scaling and absolute computational effort can be reduced even further. As for VCC, and with even lower computational cost, linear scaling can be obtained if the mode–mode interactions are only local when proceeding to systems with many degrees of freedom. Our new VSCF approach is based on a second quantization formulation.¹³ The second quantization formulation of the many body problem was decisive for the development of the many-mode VCC approach. This work is the first detailed second quantization based realization of a VSCF implementation.

There are a few other perspectives on fast VSCF methods. A new approach for the construction of potential energy surfaces (PESs) denoted adaptive density guided approach¹⁴ (ADGA) uses VSCF one-mode functions to construct one-mode densities which are used as auxiliary quantities in an iterative construction of the PES on a set of grids. The densities are used (i) to guide the addition of new grid points, (ii) to update the grid boundaries, and (iii) in the convergence checks of the iterative algorithm. Clearly, it is essential that the VSCF equations can be solved very efficiently to avoid overhead in this procedure. In addition to relying on the VSCF method, the final PES generated using ADGA may also provide savings in the vibrational structure calculations due to a more compact representation of the PES. Although our main focus will be on the VSCF algorithm itself, this paper also discusses further how the ADGA can provide additional savings with respect to both PES construction and vibrational wave function calculations using both VSCF and post-VSCF methods.

The number of vibrational states increases strongly with the size of the system. For larger molecules and significant temperatures, the population of many excited vibrational states introduces additional contributions to molecular properties in a thermodynamic framework. VSCF can also be a very useful tool in this respect. With the algorithms of this work VSCF is now so fast that it is in fact conceivable to calculate many millions of states explicitly. Furthermore, a recently introduced approach for combining anharmonic wave functions with statistical mechanics has the determination of the VSCF reference state as the rate limiting step.¹⁵

Fast VSCF methods are thus open for calculating quantum anharmonic partition functions and temperature-dependent vibrational contributions to properties.¹⁵

In section 2 we describe the theory behind our approach. We begin with a brief account of the construction and form of the Hamiltonian since that is used later. However, the choice and construction of the coordinates are not discussed in any detail. The CPU times and scalings discussed in this paper will focus on the anharmonic vibrational wave function step. The construction of the PES can certainly be the rate determining step in many calculations, but this depends on the cost of single points (high-accuracy correlated ab initio, density functional theory (DFT), semiempirical, or even classical force field) and only the number of single-point evaluations are discussed in this work. After this background we discuss a second quantization formulation of VSCF and an accompanying implementation. This includes the active terms algorithm and various additional steps taken to reduce scaling and absolute cost. All these aspects are then explored in test calculations on all fundamental vibrations in polyaromatic hydrocarbons (PAHs) of increasing size. The computational details are described in section 3, and the results are discussed in section 4. Finally, in section 5 we give a summary and outlook.

2. Theory

2.1. Representation of the Hamiltonian. In mass-weighted normal coordinates, the rovibrational Hamiltonian,

$$H = T + V \quad (1)$$

is given by the Watson operator.¹⁶ In the simplest case where the interaction between rotation and vibration is neglected, the kinetic energy operator is approximated as a sum of one-mode operators, $T = -(1/2)\sum_m d^2/dq_m^2$. More generally, one can include the terms accounting for vibrational angular momentum and effective inverse moments of inertia which are of importance in some systems. However, this is only a minor detail in the context of this work and will not be considered further here.

The construction of the PES, V , is an area of much research; see, e.g., ref 17 and references therein. Normal modes are nonlocal by construction and may conveniently reduce some couplings in size, but the PES described in nonlocal coordinates may not exhibit in a useful way the expected decay of the size of couplings with distance. A converging series of approximate PESs is introduced,

$$V^{(1)}, V^{(2)}, \dots, V^{(M)} \quad (2)$$

where $V^{(1)}$ corresponds to the uncoupled anharmonic oscillator approximation, $V^{(2)}$ includes all couplings among pairs of modes as well, etc. Eventually, the fully coupled M -mode PES, $V^{(M)}$, may be recovered. The use of such restricted mode coupling expansions has become widespread.^{18–23} In practical terms, this means that the PES is written as a sum of low-dimensional subpotentials,

$$V = \sum_m \bar{V}^m \quad (3)$$

In eq 3 the subpotentials $\bar{V}^{\mathbf{m}}$ are functions only of the modes given in the mode combination (MC) \mathbf{m} and defined such that the function is zero if any of the corresponding coordinates are zero. For instance, \bar{V}^{m_1, m_2} embodies the true two-mode coupling between modes m_1 and m_2 , and it is related to the original potential function as $\bar{V}^{m_1, m_2}(q_{m_1}, q_{m_2}) = V(\dots, 0, q_{m_1}, 0, \dots, 0, q_{m_2}, \dots) - V(\dots, 0, q_{m_1} = 0, 0, \dots, 0, q_{m_2}, \dots) - V(\dots, 0, q_{m_1}, 0, \dots, 0, q_{m_2} = 0, \dots)$.

It is computationally convenient to work with a Hamiltonian in the sum over products (SOP) form,

$$H = \sum_{t=1}^{N_t} c_t \prod_{m=1}^M h^{m,t} = \sum_{t=1}^{N_t} c_t \prod_{m \in \mathbf{m}^t} h^{m,t} = \sum_{t=1}^{N_t} c_t H^{\mathbf{m}^t} \quad (4)$$

where N_t is the number of terms in the operator and \mathbf{m}^t is a MC denoting the set of modes that have one-mode operators $h^{m,t}$ different from the unit operator in that particular term.

It has previously been shown how a Hamiltonian in the form of eq 4 can be very useful for efficient implementation of quantum dynamics codes, e.g., within the multiconfigurational time-dependent Hartree (MCTDH) framework²⁴ and for VCC wave functions.¹² Clearly, the Hamiltonian is not directly given in the SOP form, and it must be part of our numerical procedure to construct it in this way.

The simplest method is based on a Taylor expansion of the PES around the equilibrium geometry which clearly provides the PES in the required SOP form. Another method involves the calculation of the PES on a set of grid points, and an analytical representation of the PES is then obtained by a least-squares fitting with a multivariate polynomial function of sufficiently high degree.¹⁷ The combined use of the restricted mode coupling expansion, eq 3, and the fitting of the low dimensional subpotentials to a direct product polynomial basis ensures that the PES is eventually given in the SOP form, eq 4. A minor technical detail relevant later is that, for numerical stability, the fitting is done in frequency scaled normal coordinates, $\tilde{q}_i = (\omega_i)^{1/2} q_i$, ω_i being the harmonic frequency of the i th vibrational mode.

For both the Taylor expansion approach and the grid-based approach described above, the one-mode operators are simply normal coordinates in powers up to the degree of the polynomial expansion, D , i.e., q_m^i with $i = 1, 2, \dots, D$, as well as second-order derivatives, $(\partial^2)/(\partial q_m^2)$. The integrals required for the implementation of VSCF using a Hamiltonian written in the SOP form are one-mode integrals of the type

$$h_{ijm}^{m,t} = \langle \phi_{im}^m(q_m) | h^{m,t} | \phi_{jm}^m(q_m) \rangle \quad (5)$$

Different ways of handling these integrals have been implemented depending on the form of the PES and the chosen basis set; see refs 14 and 17. In any case, there are only a few integrals per mode and the integral evaluation is one-dimensional and can thus be done simply and fast. In fact, due to the choice of a SOP operator, the integral part becomes independent of the dimensionality of the PES. The integral part always scales linearly with respect to the size of the system with a very low prefactor. The calculation and

storage of the one-mode integrals are therefore never limiting factors in the calculations and will not be discussed any further.

The above procedures for obtaining analytical representations of the potential part of the vibrational Hamiltonian relies on the ability to perform accurate fits to multidimensional grids of points. For systems with strongly coupled modes, this might not be straightforward, but the ability to use fairly high polynomial degrees (say on the order of 14) provides some flexibility. The problem is mentioned here for completeness. We also note in passing that other approaches circumventing this step are widespread.^{18,25,26}

2.2. Adaptive Density-Guided Approach for the PES Construction. The ADGA was developed to provide a robust, accurate, and black-box procedure for constructing molecular PESs. ADGA uses the reduced density of the nuclear wave function to iteratively tailor the grids (both the spatial extension and mesh) onto which each of the potential energy functions are evaluated. By using the quantity $\rho V^{\mathbf{m}}$, where ρ is the density of the VSCF wave function and $V^{\mathbf{m}}$ is the potential energy function for the given MC, \mathbf{m} , the MCs containing modes which are not strongly coupled will be given a compact representation based on only a few single-point calculations. More important couplings will be given a more elaborate form based on many more sampling points. As a consequence, the number and placement of the single-point energy calculations are optimized, thus reducing considerably the CPU time spent in the construction of the PES and potentially improving accuracy at the same time. As an additional advantage, the more compact representation of in particular weak couplings can potentially improve the computational scaling of the vibrational wave function calculations. For instance, a weak two-mode coupling may in the most favorable case be represented simply through the terms $q_i q_j$, $q_i^2 q_j$, $q_i q_j^2$, and $q_i^2 q_j^2$, which is obviously computationally cheaper to handle than a high-order polynomial approximation. In fact, as the system grows larger, one can expect that the ratio between the number of weak and strong mode couplings increases and it is therefore essential to have a method capable of approximating with minimal cost the weak couplings. For a complete overview of the adaptive procedure we refer to refs 14 and 27.

2.3. Vibrational Self-Consistent Field Theory. We begin our derivation by noting that whereas previous formulations of VSCF theory have been done in first quantization, we choose to work in the second quantization formalism introduced in ref 13. Note that this second quantization formalism is different from the harmonic oscillator step-up/step-down operator formulation sometimes used in vibrational theory. The advantages of second quantization in relation to VSCF will become apparent during the course of the derivation.

The VSCF ansatz for the wave function of a system with M modes is written as

$$|\text{VSCF}\rangle = \exp(\kappa) |\Phi_i\rangle = \exp\left(\sum_{m=1}^M \sum_{p^m q^m} \kappa_{p^m q^m}^m E_{p^m q^m}^m\right) |\Phi_i\rangle \quad (6)$$

The reference state is given by

$$|\Phi_i\rangle = \prod_{m=1}^M a_{im}^{m\dagger} |\text{vac}\rangle \quad (7)$$

where \mathbf{i} is a vector indicating for each mode which modal is occupied in the reference state, and

$$E_{pmqm}^m = a_{pmqm}^{m\dagger} a_{pmqm}^m \quad (8)$$

The basic creation and annihilation operators, $a_{rm}^{m\dagger}$ and a_{rm}^m , satisfy the commutator relations

$$[a_{rm}^m, a_{sm'}^{m'\dagger}] = \delta_{mm'} \delta_{rmsm'} \quad (9)$$

$$[a_{rm}^m, a_{sm'}^{m'}] = [a_{rm}^{m\dagger}, a_{sm'}^{m'\dagger}] = 0 \quad (10)$$

and the killer condition,

$$a_{rm}^m |\text{vac}\rangle = 0 \quad (11)$$

The operator κ is antihermitian such that $\exp(\kappa)$ is unitary and the exponential prefactor therefore generates rotations among the modals.

The optimal VSCF modals are obtained by invoking the variational principle on the modal rotation parameters, κ_{pmqm}^m , of the VSCF energy,

$$E_{\text{VSCF}} = \langle \Phi_i | \exp(-\kappa) H \exp(\kappa) | \Phi_i \rangle \quad (12)$$

giving

$$0 = \frac{\partial}{\partial \kappa_{pmqm}^m} \langle \Phi_i | \exp(-\kappa) H \exp(\kappa) | \Phi_i \rangle \quad (13)$$

By inserting the expression for the κ operator, eq 6, into eq 13, one obtains straightforwardly, for $\kappa = 0$, that the criterion for having an optimal $|\Phi_i\rangle$ state is

$$0 = \langle \Phi_i | [H, E_{pmqm}^m] | \Phi_i \rangle \quad (14)$$

This is the VSCF analogue of the Brillouin condition. An effective mean-field operator for mode m , $F_{rm}^{m,i}$, may be introduced with matrix elements¹³ (notice that there is an unfortunate sign error in eq 59 of ref 13).

$$F_{rm}^{m,i} = \langle \Phi_i | [[a_{rm}^m, H], a_{sm}^{m\dagger}] | \Phi_i \rangle \quad (15)$$

By applying the basic second quantization commutator relations, the nonredundant elements, corresponding to occupied-virtual rotations, are given by

$$F_{imqm}^{m,i} = \langle \Phi_i | [H, E_{qmim}^m] | \Phi_i \rangle \quad (16)$$

$$F_{qmim}^{m,i} = -\langle \Phi_i | [H, E_{imqm}^m] | \Phi_i \rangle \quad (17)$$

where we have used i^m for occupied and a^m for virtual modals. The $\mathbf{F}^{m,i}$ matrix elements are thus directly related to the VSCF gradient terms, eq 14. A zero gradient for mode m may be obtained by diagonalizing the $\mathbf{F}^{m,i}$ matrix,

$$\mathbf{F}^{m,i} \mathbf{C}^m = \mathbf{C}^m \boldsymbol{\epsilon}^m \quad (18)$$

for all modes. In eq 18, \mathbf{C}^m is a matrix containing the current set of optimized modals while $\boldsymbol{\epsilon}^m$ is a diagonal matrix holding

the corresponding modal energies. An outline of our VSCF procedure will be given in a subsequent section.

At this point, we note that the computationally demanding part of the self-consistent scheme is the construction of the $\mathbf{F}^{m,i}$ matrix which involves the Hamiltonian. The Hamiltonian in SOP form, see eq 4, can in second quantization be represented as

$$H = \sum_t c_t \prod_{m' \in \mathbf{m}^t} \sum_{p^{m'} q^{m'}} h_{p^{m'} q^{m'}}^{m',t} E_{p^{m'} q^{m'}}^{m'} \quad (19)$$

where the integrals, $h_{p^{m'} q^{m'}}^{m',t}$, are given by eq 5. The effective operator in eq 15 may thus be written

$$F_{rm}^{m,i} = \sum_t c_t \langle \Phi_i | [[a_{rm}^m, \prod_{m' \in \mathbf{m}^t} \sum_{p^{m'} q^{m'}} h_{p^{m'} q^{m'}}^{m',t} E_{p^{m'} q^{m'}}^{m'}], a_{sm}^{m\dagger}] | \Phi_i \rangle \quad (20)$$

This may be simplified by using the commutator relations

$$[A, B_1 B_2 \dots B_N] = \sum_{i=1}^N B_1 B_2 \dots B_{i-1} [A, B_i] B_{i+1} \dots B_N \quad (21)$$

$$[[a_{rm}^m, E_{p^{m'} q^{m'}}^{m'}], a_{sm}^{m\dagger}] = \delta_{rm p^{m'}} \delta_{sm q^{m'}} \delta_{mm'} \quad (22)$$

the latter of which follows directly from eqs 9–11.

From the $\delta_{mm'}$ in eq 22, it follows that if mode m is not contained in term t , it simply evaluates to zero and one needs not to consider that term in the construction of the $\mathbf{F}^{m,i}$ matrix. This defines our active terms algorithm: In the process of evaluating the effective $\mathbf{F}^{m,i}$ operator, we partition the terms of the Hamiltonian into two sets. The first set contains terms which are active for mode m , i.e., have a nonzero double commutator or, equivalently, have a nonunit one-mode operator for that mode. The other set contains the remaining terms which are inactive, i.e., only contain the unit operator for mode m . Mathematically, we are thus working with two sets of operator terms, $\{t_{\text{act}} | t: \mathbf{m}^t \cap \{m\} = \{m\}\}$ and $\{t_{\text{inact}} | t: \mathbf{m}^t \cap \{m\} = \{\}\}$.

For the active terms, eq 20 finally evaluates to

$$\begin{aligned} F_{rm}^{m,i} &= \sum_{t \in \{t_{\text{act}}\}} c_t \prod_{m' \in \mathbf{m}^t \setminus m} h_{im' q^{m'}}^{m',t} \times \\ &\quad \sum_{p^{m'} q^{m'}} h_{p^{m'} q^{m'}}^{m',t} \langle \text{vac} | a_{im}^m [[a_{rm}^m, E_{p^{m'} q^{m'}}^m], a_{sm}^{m\dagger}] a_{im}^{m\dagger} | \text{vac} \rangle \\ &= \sum_{t \in \{t_{\text{act}}\}} z^{m,t} h_{rm}^{m,t} \end{aligned} \quad (23)$$

where we have introduced the effective factor

$$z^{m,t} = c_t \prod_{m' \in \mathbf{m}^t \setminus m} h_{im' q^{m'}}^{m',t} \quad (24)$$

We now turn briefly to first quantization where the mean-field operator for mode m assumes the form

$$F_Q \mathbf{F}^{m,i} = \langle \prod_{m' \neq m} \phi_{im'}^{m'} | H | \prod_{m' \neq m} \phi_{im'}^{m'} \rangle \quad (25)$$

Here, the integration is understood to be only over the $M - 1$ other degrees of freedom. For a SOP operator in first quantization, eq 4, this leads to the following matrix elements,

$${}^{FQ}F_{um,vm}^{m,i} = \langle \chi_{um} | {}^{FQ}\mathbf{F}^{m,i} | \chi_{vm} \rangle = \sum_t c_t \langle \chi_{um} | h_{um,t}^{m,i} | \chi_{vm} \rangle \prod_{m' \in \mathbf{m}' \setminus m} h_{im',im'}^{m',t} \quad (26)$$

where $h_{um,t}^{m,i}$ is a one-mode operator working on mode m . In eq 26 it is assumed that the modals are given as a linear combination of primitive basis functions, χ_{um} ; see, e.g., ref 10. If the Hamiltonian is partitioned into active and inactive terms, the following contributions to the ${}^{FQ}\mathbf{F}^{m,i}$ matrix are derived, assuming normalized basis functions,

$${}^{FQ}F_{um,vm}^{m,i,[\text{act.}]} = \sum_{t \in \{t_{\text{act.}}\}} z^{m,t} h_{um,t}^{m,i} \quad (27)$$

$${}^{FQ}F_{um,vm}^{m,i,[\text{inact.}]} = \delta_{um,vm} \sum_{t \in \{t_{\text{inact.}}\}} c_t \prod_{m' \in \mathbf{m}'} h_{im',im'}^{m',t} \quad (28)$$

i.e., the active part is the same as the second quantization effective operator $\mathbf{F}^{m,i}$; see eq 23. The inactive part, which is absent in the second quantization operator defined by eq 15, merely adds a constant to the diagonal. This constant contribution may be safely neglected in the course of the optimization since a constant added to the diagonal of a matrix does not affect its eigenvectors. Thus, one can introduce the same algorithm as in second quantization. However, in the latter case, the terms inactive for a given mode are naturally found not to contribute to the optimization.

2.4. Active Terms VSCF Algorithm. The optimization of the VSCF reference state may proceed in many ways. In this paper we pursue a direct first-order algorithm based upon eqs 14–18. Second-order algorithms can be constructed on the basis of the Hessian, i.e., the second-order derivatives of the VSCF energy expectation value, eq 12. However, so far we have found the first-order procedure to be sufficiently stable. Our algorithm is based on a simple structure where we solve the VSCF eigenvalue equations for one mode at a time. This requires the construction of the VSCF mean-field operator, $\mathbf{F}^{m,i}$, and its subsequent diagonalization. This defines a new set of one-mode functions for this particular mode. The new occupied one-mode function is used in the construction of the VSCF mean-field operators for the other modes.

Thus, the algorithm for solving the VSCF equations proceeds as follows:

```

Loop over VSCF iterations
  Loop over all modes  $m$ 
    Construct the  $\mathbf{F}^{m,i}$  matrix
    Diagonalize  $\mathbf{F}^{m,i}$ 
    Update  $h_{im',im'}^{m',t}$  list
  Calculate the VSCF energy and test for convergence
  
```

The diagonalization is in the space of one-mode functions for a single mode and the matrix dimension is therefore $N^m \times N^m$, where N^m is the size of the one-mode basis used for the expansion of the modals for mode m . Thus, it is a local diagonalization independent of the size of the system with a computational cost depending only on the size of the basis set for each single mode. The update step calculates the integrals, $h_{im',im'}^{m',t}$, for the occupied level of each mode such that these are readily available when needed in the calculation of $\mathbf{F}^{m,i}$ for other modes as well as the energy,

$$E = \sum_t c_t \prod_{m \in \mathbf{m}'} h_{im',im'}^{m',t} \quad (29)$$

Given the Hamiltonian operator in the SOP form, eq 4, the active terms part for calculating $\mathbf{F}^{m,i}$ in the self-consistent algorithm sketched above, proceeds as follows: We initially determine for each mode m the corresponding set of active terms in the Hamiltonian. Given this set, we, for each mode m , make a pass through the active terms for m . For each term we first calculate the $z^{m,t}$ factor by looping through the modes in the particular term, excluding the target mode m . After the $z^{m,t}$ factor has been constructed, the relevant one-mode integrals for mode m are multiplied with $z^{m,t}$ and the result added to $\mathbf{F}^{m,i}$.

To set the above considerations into perspective, we note that a M mode Hamiltonian which couples all pairs of modes through its potential part has $M(M-1)/2$ couplings. For such an operator, only $M-1$ couplings will be active in a given mode; the remaining $(M-1)(M-2)/2$ couplings are inactive. Thus, the computational cost of constructing the $\mathbf{F}^{m,i}$ matrix is reduced by a power of M simply by construction as the inactive terms need not be considered. Indeed, this order of reduction of the computational effort is gained for all potentials, regardless of the order of the coupling in the Hamiltonian; i.e., the computational complexity for the construction of a $\mathbf{F}^{m,i}$ matrix involving a N -mode coupled Hamiltonian is reduced by the active terms algorithm as

$$\mathcal{O}(M^N) \rightarrow \mathcal{O}(M^{N-1}) \quad (30)$$

M of these matrices must be constructed in each iteration. Thus, the total computational complexity decreases from $\mathcal{O}(M^{N+1})$ to $\mathcal{O}(M^N)$.

Assume that the number of active terms for each mode in the system is limited. More precisely, each mode m is coupled directly to a limited set of modes much smaller than the total set of modes. This means that there are many other modes, m' , having no terms containing operators for both m and m' . If the active terms algorithm is employed, the time required for construction of the $\mathbf{F}^{m,i}$ matrix is thus expected to be fairly constant with respect to the size of the system though still linear in the number of active terms per mode. Thereby, the scaling of the whole VSCF algorithm becomes linear in the number of modes. In total, the computational scaling of the active terms implementation scales roughly as the number of modes times the number of active terms per mode.

2.5. Screening. It is possible at various stages in the VSCF algorithm to avoid calculation of contributions that are numerically negligible.

Most trivially, terms in the Hamiltonian with c_t coefficients less than a certain threshold can be neglected. This is relevant since the automatic procedures for determining the PES may generate terms with essentially zero coefficients. This form of screening is employed already when reading in the operator, before the VSCF calculation.

In relation to the algorithm outlined above, screening on the basis of the magnitude of the $z^{m,t}$ factor in eq 24 has also been implemented. If the absolute value of $z^{m,t}$ times the norm

(square root of the sum of element norms squared) of the $h^{m,t}$ integrals is less than a certain threshold times the expected norm of the target quantity, $\mathbf{F}^{m,\text{act}}$, the scaling of the $h^{m,t}$ integrals and addition of the contribution to the $\mathbf{F}^{m,i}$ matrix are avoided. The latter method defines a more rigorous screening strategy but on the other hand also requires significantly more computational work compared to the screening on the Hamiltonian coefficients. We will in the following investigate both of these types of screening as well as a combination of the two.

2.6. Combination of Terms in the Hamiltonian. Yet another method for reducing the number of terms in the Hamiltonian, and thereby the computational cost, may be introduced by combining terms in the operator. Consider the Hamiltonian in eq 4. Each term is a product of one-mode operators. The terms can be grouped into sets where only the operator for a single mode differs between the terms. Each of these sets can be reduced to a single term by isolating the mode where the difference occurs, for instance for modes 0 and 1:

$$c_1 q_0^n q_1^a + c_2 q_0^n q_1^b + c_3 q_0^n q_1^c = q_0^n (c_1 q_1^a + c_2 q_1^b + c_3 q_1^c) \quad (31)$$

Here three terms have been reduced to one by introducing an effective one-mode operator that is simply a linear combination of the original ones. As a realistic example, consider a two-mode Hamiltonian with simple kinetic energy operators given by the second derivatives of the normal coordinates and a Taylor expanded PES of order D . In this case the individual operators are d^2/dq^2 , and q^n , with $n = 1, 2, \dots, D$. By combining terms, the number of one-mode operator terms is reduced from $M(D + 1)$ to M . The number of two-mode operator terms is reduced from $M(M - 1)D(D - 1)/4$ to $M(M - 1)D/2$, i.e., by a factor of $(D - 1)/2$. We note here that the Taylor PESs are usually of low polynomial order, and more significant savings may be observed for a grid-based potential. The computational cost for this reduction comes in terms of the extra integrals needed to be handled corresponding to the combined one-mode operators. These integrals can be stored or calculated on the fly.

Combining terms reduces the total number of terms in the Hamiltonian. The CPU time depends rather directly on the number of terms per mode so there are potentially significant savings in CPU time by combining terms. We note that the computational scaling with respect to the size of the system is not changed by combining operator terms. The drawback of combining terms is that it introduces in one form or another additional storage and logic in the handling of the operator information.

2.7. Program. The VSCF method is implemented in the MidasCpp (Molecular Interactions, Dynamics and Simulation in C++/Chemistry Program Package) program.²⁸ The MidasCpp program also includes the discussed static and adaptive grid methods for generating potential energy and property surfaces. Interfaces to widely known electronic structure programs including DALTON, ACESII, CFOUR, and GAMESS are available in order to perform the electronic

structure calculations needed for the construction of potential energy and molecular property surfaces.

3. Computational Details

In this study, we have investigated polyaromatic hydrocarbons (PAHs) consisting of 1–24 fused benzene rings with at most four rings in each row. The PAHs will be denoted PAH n , $n = 1, 2, \dots, 24$ corresponding to the number of fused benzene rings in the molecule. In Figure 1 we present a few examples of PAH structures.

The PAHs have been optimized at the PM3 level^{29,30} using the GAMESS program.^{31,32} A normal mode vibrational analysis has been performed by building the Hessian matrix numerically from analytical gradients. A step size of 5×10^{-4} au has been used. The MidasCpp suite of programs has been used to construct the PESs through an interface to the GAMESS quantum chemistry program. Both the static grid method as well as ADGA have been used. In the static grid method, $1618_{3/4}$ sets of coarse grid points have been used (see ref 17 for notation). To these grids, a number of additional points have been added by spline interpolation. Analytical representations of the PESs have been obtained via least-squares fitting with a multivariate polynomial function of 12th degree and using a cutoff of 12 in the bidimensional fittings. No use of point group symmetry was made.

The thresholds used for the construction of the PESs with the ADGA procedure are as follows: the one-mode surfaces were converged with $\epsilon_{\text{rel}} = 1 \times 10^{-2}$ and $\epsilon_{\text{abs}} = 1 \times 10^{-6}$, while the two-mode surfaces were converged with $\epsilon_{\text{rel}} = 5 \times 10^{-2}$ and $\epsilon_{\text{abs}} = 5 \times 10^{-6}$ (see ref 14 for details). The boundaries of the one-mode grids were iteratively determined by requiring that 99.9% of the mean density constructed from the three lowest vibrational states for each vibrational mode was included in the boundaries of the one-mode grids.

As for the static grid approach, the maximum polynomial degree used for the fitting of the surfaces is 12. However, in the early cycles of the iterative procedure, when few evaluation points are available, the maximum degree of the fitting polynomials are reduced to $n - 1$ with n being the number of evaluation points.

The basis set used during the VSCF calculations (both during the ADGA and in the analysis of the VSCF and VCC performances) consists of 13 harmonic oscillator functions for each of the vibrational modes corresponding to vibrational quantum numbers $v = 0, 1, \dots, 12$.

It should be noted that the energies and wave functions obtained from the VSCF calculations differ slightly between the ADGA and static grid PESs. The mean absolute deviation (MAD) between fundamental excitation energies is of the order of 1 cm^{-1} for all molecules.

The timings presented in the following are, with the exception of the results for the duplicated PAH7 systems, obtained on SUN Fire x2100 dual core servers (2.2 GHz, 2GB memory) and refer to one iteration in the VSCF part; i.e., PES construction and other time-consuming steps are not treated.

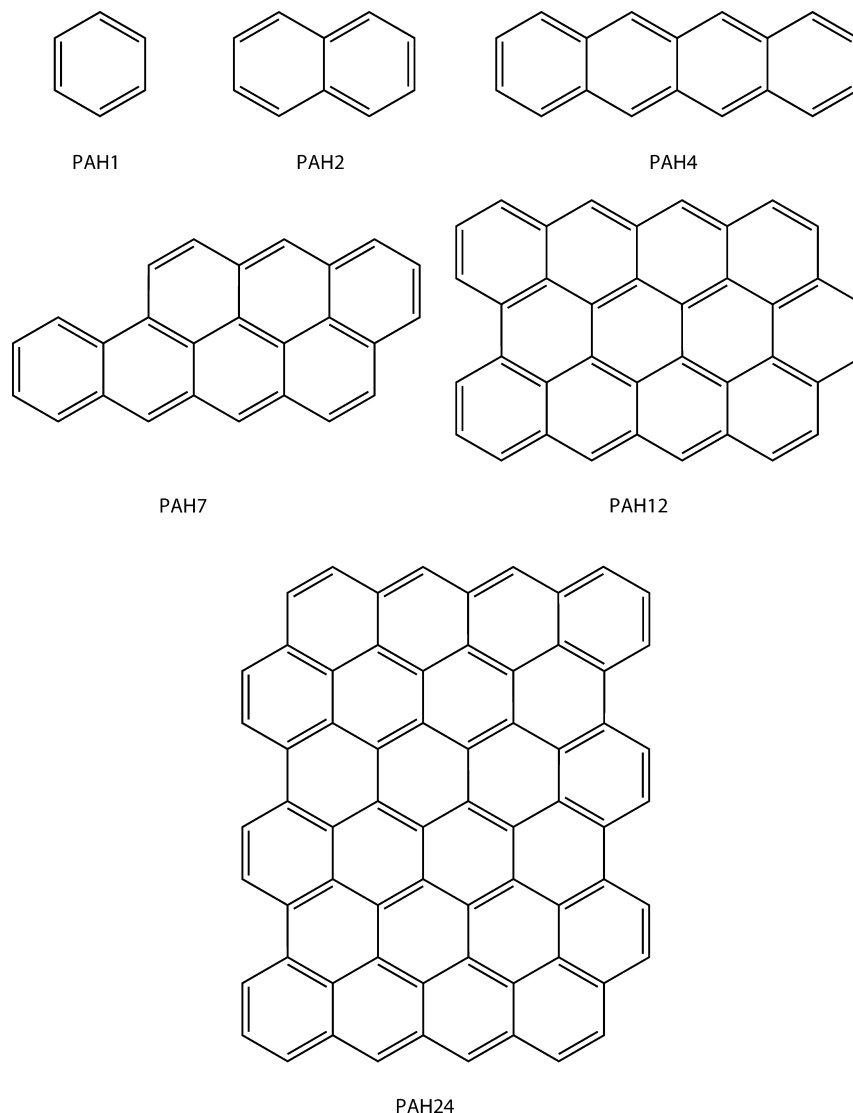


Figure 1. Examples of polyaromatic hydrocarbons.

4. Sample Calculations: Polyaromatic Hydrocarbons

In this section we describe some sample calculations. The VSCF approximation as such and most of its limitations have been extensively discussed in the literature, and we shall here primarily discuss aspects relating to our new implementation. Thus, the focus is on timings for systems of systematically increasing size. The PAHs define a class of molecules that can be extended in a systematic fashion with the normal coordinates still being able to provide a reasonable description of the systems.

4.1. PES Setup. In Figure 2 we present, as a function of system size, the number of terms in the Hamiltonian and the number of required single-point evaluations using the static grid approach and ADGA.

The static grid method provides a simple quadratic increase in the number of single-point evaluations and the number of terms in the Hamiltonian. This follows trivially from the number of mode-coupling pairs, $(1/2)M(M - 1)$, each of which requires a constant number of evaluation points and adds a constant number of terms to the Hamiltonian. In

ADGA, the same number of mode-couplings is handled but the number of single-point evaluations and terms varies among the couplings. From the inspection of Figure 2 it is clear that ADGA is more efficient than the static grid method in terms of single-point evaluations. The saving in single-point evaluations increases with increasing system size from 17% for PAH1 (benzene) to 77% for PAH24. Turning to the number of terms in the Hamiltonian, ADGA again offers quite large savings. For the largest systems investigated here, the analytical representation of the potential obtained with the ADGA contains only 12% of the number of terms present in the static grid Hamiltonian. This in turn provides computational savings in the vibrational structure calculations. The saving is significant for molecules of the size of PAH24 where the number of terms may otherwise easily exceed 1 million even for two-mode coupled potentials.

4.2. Scaling of Native VSCF versus Active Terms Algorithm. To investigate the performance of the active terms algorithm relative to the native VSCF algorithm in a simple setting, we initially use the static grid PESs which

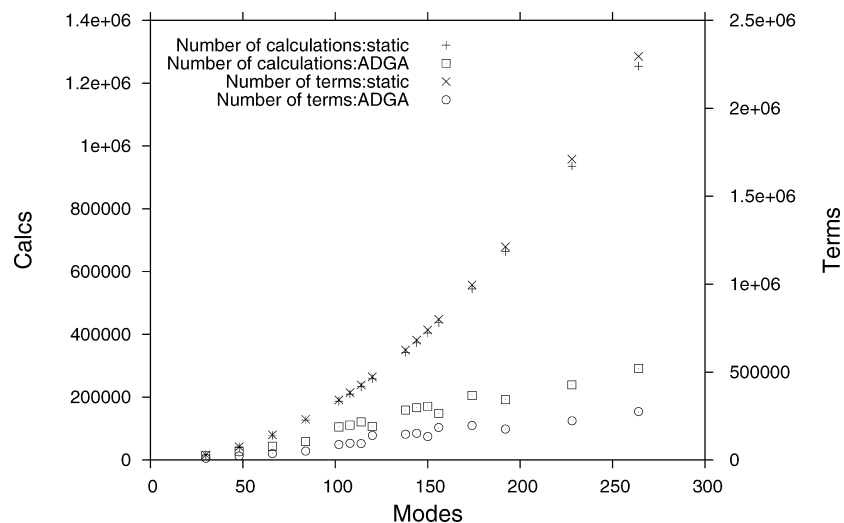


Figure 2. Number of single-point calculations (left) and the number of terms in the potential (right) in the static grid and ADGA potentials as a function of the number of vibrational degrees of freedom.

have a fixed number of terms per mode-coupling irrespective of the size of the system.

In the following, we assume that the CPU time for one VSCF iteration follows a simple equation of the type

$$t = 10^A M^B \quad (32)$$

or

$$\log t = A + B \log M \quad (33)$$

where M is the number of modes and A and B are fitting parameters. In the following we report computational scaling B and the prefactor 10^A . This allows for a very simple identification of the computational scaling as seen in Figure 3 which reports a log–log plot of the CPU time as a function of system size for the native and active terms algorithms. Linear least-squares fits are shown as well.

Due to the fact that the Hamiltonian couples all pairs of modes, and we in this subsection do not take any measures

to reduce the cost of evaluating all these couplings, the CPU time increases approximately proportional to some power of M as discussed in Theory. From Figure 3 it is seen that the native algorithm has a scaling of 2.6. The reason for this deviation from the expected cubic scaling is due to the fact that the leading order scaling is determined by the number of inactive terms in eq 28, which scales like M^2 (for all M modes) rather than the number of active terms in eq 27, which scales like M . However, the inactive terms are very simple to calculate (stored in memory at all times), making the prefactor on this term very low. This, in turn, results in comparable computational times for the active and inactive parts even for systems with 264 modes. The formula of eq 32 is too simple to capture this behavior.

For an operator with a mode-coupling level of two, one should obtain quadratic scaling when using the active terms algorithm. This is confirmed by the results reported in Figure 3. The difference in computational times between the active

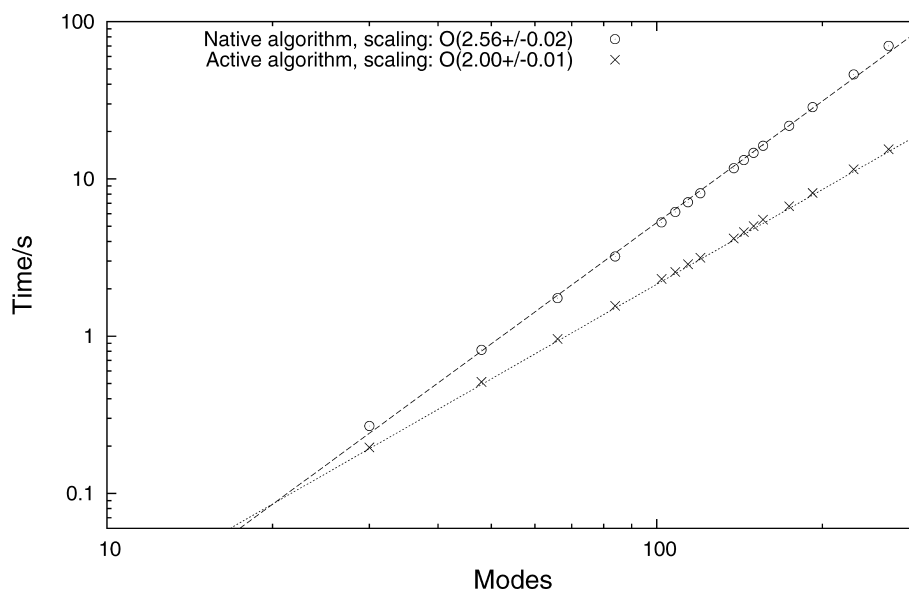


Figure 3. Time for a single VSCF iteration as a function of the size of the system (log–log scale). The broken and dotted lines represent the curves fitted to the data for the native and active terms, respectively.

Table 1. Computational Complexity of One VSCF Iteration When Screening Is Employed in the Active Terms Algorithm^a

threshold(c_i)	threshold ($z^{m,i}$)	reorder ^b	scaling	prefactor	max(MAD) ^c	max(MAXAD) ^d
		no	2.00 ± 0.00	$10^{-3.67 \pm 0.01}$		
10^{-12}		no	1.89 ± 0.04	$10^{-3.68 \pm 0.08}$	1.3×10^{-4}	5.8×10^{-3}
10^{-10}		no	1.79 ± 0.05	$10^{-3.70 \pm 0.10}$	7.5×10^{-3}	3.5×10^{-2}
10^{-9}		no	1.82 ± 0.05	$10^{-3.91 \pm 0.10}$	7.2×10^{-2}	3.6×10^{-1}
	10^{-8}	no	1.86 ± 0.05	$10^{-3.87 \pm 0.10}$	1.1×10^{-8}	7.4×10^{-8}
	10^{-6}	no	1.79 ± 0.03	$10^{-4.01 \pm 0.07}$	4.4×10^{-6}	1.6×10^{-5}
	10^{-5}	no	1.84 ± 0.04	$10^{-4.14 \pm 0.07}$	8.3×10^{-4}	1.3×10^{-4}
	10^{-4}	no	1.57 ± 0.04	$10^{-3.94 \pm 0.09}$	3.2×10^{-2}	2.1×10^{-1}
10^{-9}	10^{-5}	no	1.71 ± 0.05	$10^{-4.09 \pm 0.11}$	8.0×10^{-2}	3.6×10^{-1}
10^{-9}	10^{-4}	no	1.48 ± 0.05	$10^{-3.79 \pm 0.10}$	9.4×10^{-2}	4.4×10^{-1}
10^{-9}	10^{-4}	yes	1.80 ± 0.04	$10^{-4.29 \pm 0.12}$	8.4×10^{-2}	3.7×10^{-1}

^a The CPU time is assumed to be proportional to the number of modes to some scaling power multiplied by a prefactor. The scaling powers and the prefactors are listed in the table, given in terms of 10^A and B ; see eqs 32–33. The errors (cm^{-1}) introduced are listed as well. ^b Specifies whether reordering of the operator terms has been used. ^c Largest value among the MAD for all molecules; see text for details. ^d Largest value among the MAXAD for all molecules; see text for details.

terms algorithm and the native algorithm is thus due to the inactive terms. For PAH2, PAH6, and PAH24, the fraction of time spent in the inactive terms part is 37, 59, and 78%, respectively, clearly indicating that for larger systems the computational effort of the native algorithm is dominated by the inactive part, and for sufficiently large systems cubic scaling is obtained.

Having clearly illustrated the better performance of the active terms algorithm over the native algorithm, we will in the following only use the active terms algorithm.

4.3. Screening. To reduce the scaling, one may use several types of screening. Here we investigate the computational speedup gained by (i) screening of the c_i coefficients, (ii) screening of the contributions to $\mathbf{F}^{m,i}$ on the basis of $z^{m,i}$, and (iii) the combination of i and ii. In Table 1 the computational scalings and prefactors are presented for several thresholds of i and ii. The mean and maximum absolute deviations (MAD and MAXAD) of the VSCF fundamental frequencies with respect to the results obtained without screening were computed for all molecules, and their maximum values are presented for each threshold as well.

4.3.1. Screening of c_i . We begin our discussion by considering screening of the c_i coefficients in Table 1. In the three cases shown, the mean and maximum absolute deviations (MAD and MAXAD) of the VSCF fundamental frequencies with respect to the results obtained without screening are all below 0.5 cm^{-1} . This is certainly acceptable for VSCF fundamental frequencies. It is worth noting that many-mode correlation effects beyond VSCF and variations in the electronic structure methods for generating the individual PES points, as well as details in the construction of the PES may easily provide larger effects. Thus, 0.5 cm^{-1} is well below the accuracy expected in the full calculation. For the screening thresholds included in Table 1, the scaling is reduced compared to quadratic scaling but no clear trend is evident. Thresholds of 10^{-12} , 10^{-10} , and 10^{-9} yield scalings of 1.89, 1.79, and 1.82, respectively.

4.3.2. Screening on Contributions to $\mathbf{F}^{m,i}$ on the Basis of $z^{m,i}$. The screening on the contributions to the elements of the $\mathbf{F}^{m,i}$ matrices represents a perhaps more rigorous way of screening than the screening on the PES expansion coefficients.

In Table 1 we present the results obtained for PAH n , $n = 1–24$, using several thresholds for the screening of contributions to $\mathbf{F}^{m,i}$ by inspecting $z^{m,i}$. The computational scaling

with the system size decreases compared to quadratic scaling when increasing the screening threshold above 10^{-10} . For screening thresholds of 10^{-8} to 10^{-5} the computational scalings are rather similar and within their respective standard errors. A threshold of 10^{-4} provide a computational scaling of $M^{1.57 \pm 0.04}$, which represents a significant reduction of the unscreened quadratic computational scaling. With a threshold of 10^{-4} , the maximum MAD and MAXAD errors are 0.03 and 0.2 cm^{-1} , which is clearly acceptable for systems of this size. For lower screening thresholds, the MAD and MAXAD errors are significantly lower.

4.3.3. Combined Screening. Figure 4 illustrates the computational scaling when using a threshold of 10^{-9} for the direct screening on the c_i coefficients and a threshold of 10^{-4} for the screening of $z^{m,i}$. The MAD/MAXAD for the VSCF fundamental frequencies for each molecule relative to those obtained without any screening are included as well. For completeness, the results from the combined screening are presented in short form in Table 1.

With these thresholds, we obtain a computational scaling of $M^{1.48 \pm 0.05}$ with respect to system size. This should be compared to the quadratic scaling when not exploiting screening. The scaling of $M^{1.48 \pm 0.05}$ is seen to be lower than the scaling found when using screening on $z^{m,i}$ or c_i alone. There is some synergistic effect when employing the two types of screening simultaneously, but the effect is fairly small compared to the $z^{m,i}$ screening alone. It is worth noting that the time for performing one VSCF iteration is about a half-second for the PAH24 molecule which consists of 264 modes. The unscreened active terms algorithm in comparison took 15.4 s, while the unscreened native algorithm takes 70.0 s per iteration. The errors introduced are rather similar to the ones found for the screening on c_i alone and are considered to be acceptable. In conclusion we may, by using the new active terms algorithm together with different screening strategies, bring down the VSCF iteration time very significantly compared to the standard VSCF algorithm, 2 orders of magnitude for a 264 mode system.

In addition to screening, one may consider the combination of operator terms as described in Theory. In Table 1 we include the scaling, prefactor, and errors obtained when employing this trick as well. It is evident that the computational scaling does not come out quite as favorable as in the case where we just employ two types of screening. The

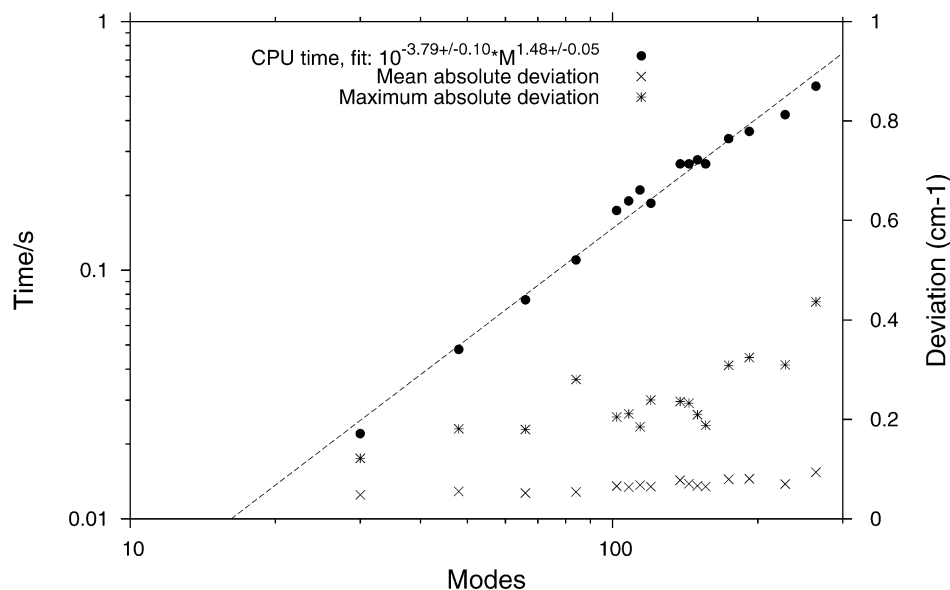


Figure 4. Time for a single VSCF iteration as a function of system size (log–log scale) when two kinds of screening are combined. The broken line represents the curve fitted to the CPU times.

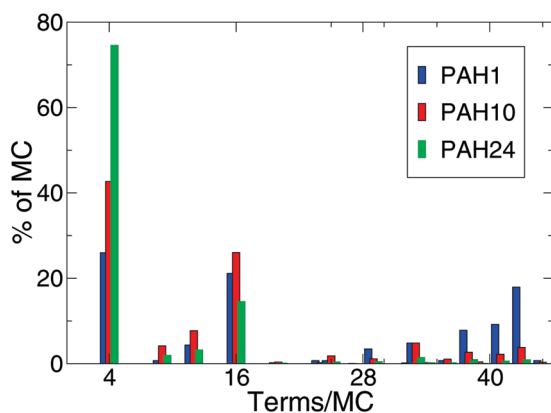


Figure 5. Distribution of operator terms per MC for PAH1, PAH10, and PAH24.

reason for this is the fact that lower fractions of the $z^{m,i}$ coefficients are screened away when employing the combination of operator terms. This trick generates more operator terms, and evidently more of these have nonnegligible contributions. For PAH10, the percentages of terms screened away with and without combination of operator terms are 70 and 84%, respectively, for the VSCF ground state.

4.4. ADGA PESs. The PESs constructed with the ADGA are particularly suitable for larger systems since, as discussed above, the ADGA is able to provide a more compact representation of weak couplings compared to a static grid approach. In this section we examine the performance of VSCF using these PESs. As stated in a previous section, a given two-mode MC may be approximated by as few as four terms in the most favorable case. In Figure 5 we present the distribution of operator terms per MC. Interestingly, the percentage of MCs which are represented by only four terms in the operator increases with increasing system size. This is of course intimately related to the savings in the number of single-point calculations observed in ADGA as compared to the static grid approach. For instance, only four single-point calculations are needed in the simplest case of four

terms in a coupling term. For PAH24, the biggest system tested, the percentage of MCs represented by four or 16 terms amounts to more than 90%.

At this point we note that the simple computational scaling formula, eq 32, is not strictly valid when using the ADGA, since the polynomial degree is allowed to adjust to the number of single-point evaluations. However, due to the very simple nature of this way of analyzing the results, we choose to use it for ADGA results as well.

The computational scaling obtained for the ADGA PESs is shown in Figure 6. A computational scaling of $M^{1.52 \pm 0.05}$ is obtained, with a significant reduction in the computational cost. One should also note that the asymptotic standard errors obtained in the fitting procedure are sufficiently small to justify the use of eq 32 in the fitting. The effect of the screening on contributions to the $\mathbf{F}^{m,i}$ matrices is shown in Figure 6 as well. A screening threshold of 10^{-4} on the $\mathbf{F}^{m,i}$ contributions changes the computational scaling to $M^{1.37 \pm 0.05}$, whereas a scaling of $M^{1.52 \pm 0.05}$ was found for the unscreened one. The prefactor also changes significantly, thus making the ADGA in combination with screening on $\mathbf{F}^{m,i}$ contributions very fast. The mean and maximum absolute deviations are less than 0.2 cm^{-1} , which is satisfactory for the VSCF method.

4.5. Predicted Important Coupling. A different method for screening away entire mode combinations is to employ the so-called predicted important coupling (PIC) schemes where the coupling strength of two different normal modes is estimated by their “atom-by-atom” overlap.²² In the simplest of these works, and the one used by Pele et al.,²² the criteria for judging whether a MC should be kept or neglected is based on whether the displacement vectors representing two normal coordinates introduce movement of the same atoms, though additional criteria may be introduced.

We tested the version of PIC in ref 22 (as well as others including additional criteria) but found that neglecting even a few MCs in this way resulted in large errors (mean and absolute) compared to the unscreened results. The neglect

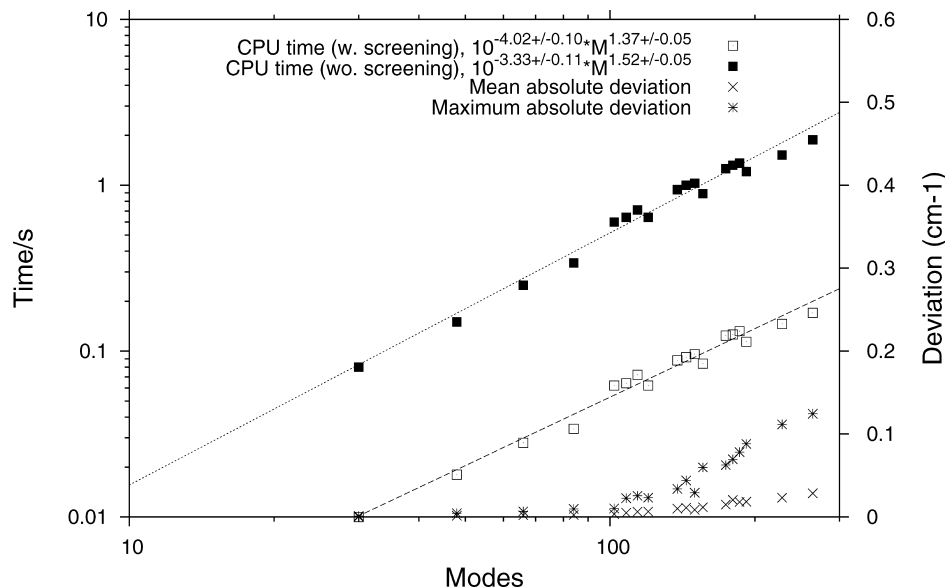


Figure 6. Time for a single VSCF iteration as a function of system size when ADGA PESs are used (log–log scale). Data both with and without screening are shown. The deviations of the screened results are provided on the right-hand scale. The broken and dotted lines represent the curves fitted to the CPU times of the screened and unscreened results.

of only 0.1 and 3% of the two-mode couplings, corresponding to specific coupling strength thresholds, resulted in MAD (MAXAD) of 0.14 (1.4) and 4.58 (40.8) cm^{-1} , respectively, for the PAH2 molecule. For a larger system represented by PAH4, neglecting 0.04 and 7% of the two-mode couplings resulted in MAD (MAXAD) of 0.16 (3.94) and 2.19 (12.5) cm^{-1} , respectively. These deviations are perhaps not too severe in comparison to the other approximations introduced, but, for these low thresholds, the computational gain in constructing the potentials as well as in the subsequent vibrational wave function calculations are rather limited.

There are certainly some nice features of the PIC schemes in terms of potentially lowering the computational scaling with respect to the number of modes. However, such intuitive schemes did not work well for the presented cases. How to remove MCs in an efficient, general, and accurate way is still an open issue.

We note that other ways of neglecting MCs are possible, for example the one advocated by Benoit.²³ Within this approach, the full PES must be calculated at a lower level of theory after which a measure of the coupling strengths are computed. On the basis of these coupling strengths MCs may be kept or neglected accordingly. The advantage of this method is that it provides a firmer measure of the coupling strengths; the drawback is that the full PES must be calculated in advance, although at a lower level of theory. This method has not been pursued in this work.

4.6. Duplicated PAH7 Molecules as a Model System.

In this section we investigate the computational scaling of the VSCF algorithm for a model system consisting of noninteracting PAH7 molecules described by the ADGA potential. Within the individual subsystems, all operator terms are maintained; i.e., we do not exploit screening. The Hamiltonian thus consists of all one-mode terms and all two-mode terms in each subunit, i.e., no terms in the Hamiltonian couple modes belonging to different mono-

mers. In this case the number of terms in the Hamiltonian is given by (as follows we assume a static grid potential for simplicity, but the same arguments may be applied to an ADGA Hamiltonian),

$$N^T = N_{\text{su}} \left(DM_{\text{su}} + \frac{1}{2} M_{\text{su}} (M_{\text{su}} - 1) D(D - 1) \right) \quad (34)$$

where N_{su} and M_{su} denote the number of subunits and the number of modes in each subunit, respectively. The total number of modes is given by $M = M_{\text{su}} N_{\text{su}}$, and hence the total number of terms is

$$N^T = M \left(D + \frac{1}{2} (M_{\text{su}} - 1) D(D - 1) \right) \quad (35)$$

The number of terms thus scales linearly with the total number of modes in the system. By the scaling arguments used in the discussion of the native and active terms algorithms (section 2.3), one may thus expect quadratic scaling of the VSCF iteration times for the native algorithm, while linear scaling should be obtained for the active terms algorithm.

Figure 7 shows the computational scaling of one VSCF iteration as a function of the number of duplicates. The plot yields a slope of 1.01 ± 0.00 in perfect agreement with linear scaling. We note that similar calculations using the native algorithm confirm the expected quadratic scaling (results not shown). In connection with this we note that the VSCF iteration time for the largest system studied here (10^6 modes) is extrapolated to be more than 2.5 CPU years using the native algorithm. In comparison, the VSCF iteration time for the active terms algorithm is just under 2 h. It is comforting to see that MidasCpp runs VSCF calculations including more than 1 million modes without having to introduce any special treatments. This aspect of the active terms algorithm is important for efficiency also in other than

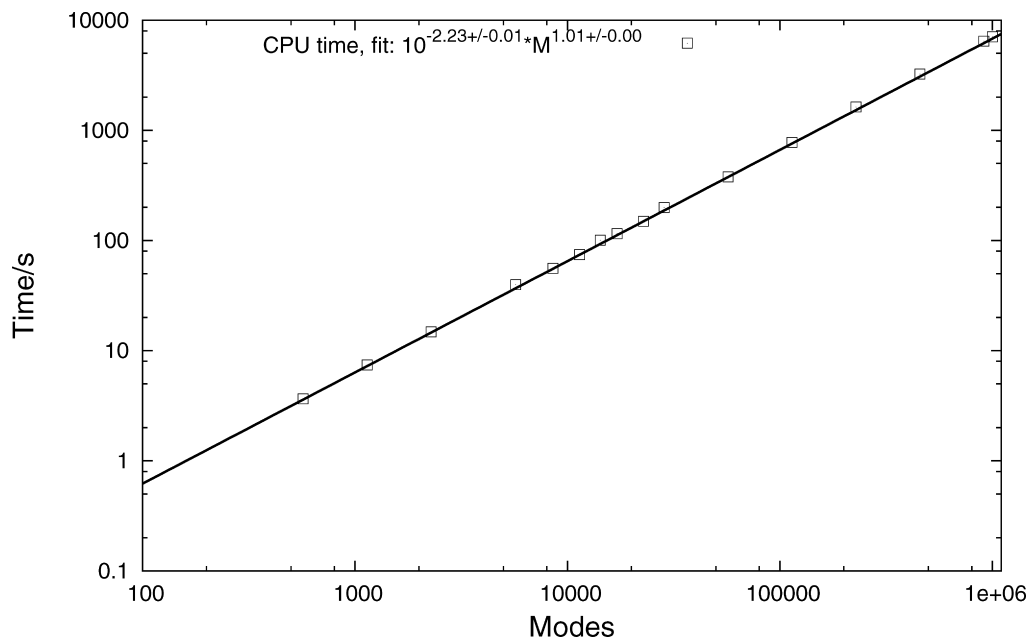


Figure 7. log–log plot of the CPU time for a single VSCF iteration as a function of the size of the system (number of modes) for duplicated PAH7 (see text).

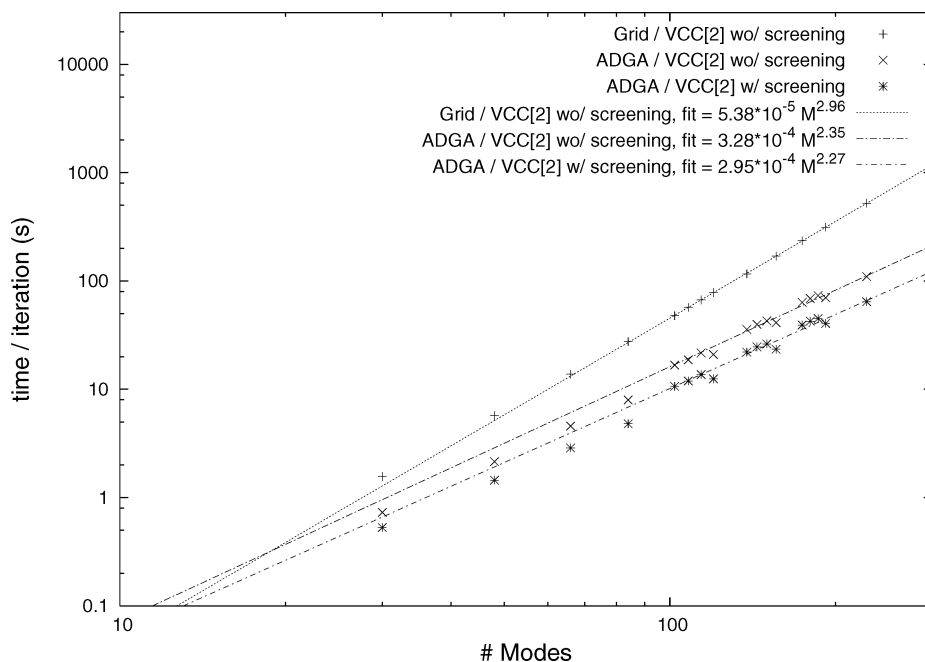


Figure 8. Scaling of the VCC[2] algorithm when applied to PAH systems described by static grid and ADGA based PESs with and without screening of the cluster amplitudes.

the present simple case. The computational cost of the active terms algorithm thus reflects the actual anharmonic coupling network.

4.7. Correlated Calculations. In a previous section it was shown how the use of ADGA PESs reduces the scaling of VSCF calculations. Though correlated calculations are not the focus of this paper, it is worthwhile to investigate whether the same is true for these kinds of calculations. For this purpose, we have used the VCC[2] algorithm reported in ref 12. For further details on basic VCC theory see ref 33. We note that the trick of combining terms in the Hamiltonian, discussed in section 2.6, is implicitly used by this algorithm. Furthermore, screening has been implemented but the details

are different from those of the VSCF algorithm since it is based primarily on the cluster amplitudes instead of the Hamiltonian terms; see ref 12 for details.

In the calculations reported here, all 13 optimal VSCF modals are included in the VCC part for each mode. Figure 8 shows the scaling of the VCC[2] algorithm applied to the series of PAHs in three different cases: Using a static grid based PES, the scaling is M^3 as previously reported.¹² More interestingly, the use of an ADGA-based PES reduces the scaling to $M^{2.35}$. The number of amplitudes in this calculation naturally remains the same as when using the static grid based PES, and the reduction is therefore simply due to the lower scaling of the number of terms in the potential part of

the Hamiltonian with respect to the system size; see Figure 2. Finally, a calculation with a screening threshold of 10^{-20} (see ref 12) shows that the screening method implemented in the VCC algorithm does not reduce the scaling but more generally improves performance. In this case the improvement is approximately 33%.

In conclusion, it is encouraging that correlated quantum mechanical calculations can be carried out for systems as large as PAH24. Furthermore, the ADGA is, also for correlated calculations, a very promising method for larger molecules.

5. Summary and Outlook

We have presented an efficient active terms algorithm for VSCF calculations. It has been demonstrated how the core part of the algorithm appears naturally by deriving the VSCF theory in second quantization formalism. It has further been demonstrated that the implementation allows for calculations on systems with many degrees of freedom. With up to a few hundred explicitly coupled degrees of freedom, a computational scaling of order $M^{1.5}$ per VSCF iteration per state was found together with a very low prefactor including two mode couplings in the Hamiltonian. The computational scaling was found to be as low as $M^{1.37}$ when using ADGA potentials in combination with screening. Sample calculations for model systems with up to 1 million degrees of freedom are reported, illustrating linear scaling when each mode interacts only with a limited set of other modes.

Even though the systems considered here are simple from some perspectives, the fact that such quantum mechanical calculations on systems of this size are possible is encouraging. In discussions of quantum methods versus classical methods it seems often to be assumed that quantum methods are inherently costly and only possible for small systems. Indeed, in many circumstances where classical mechanics is used today it is presently the only realistic option. Though there are many different bottlenecks that must be overcome in various areas of applications, this general statement need not be a valid standard assumption in the future. At least the presented very fast VSCF implementation in combination with the ADGA procedure provides a powerful tool and suggests that at least some of the conceived limitations can be removed. We will continue to work on many of the other bottlenecks of many mode quantum dynamics.

In this paper we have used normal coordinates throughout. For weakly anharmonic systems the normal coordinate harmonic oscillator description is a good reference point. However, standard normal coordinates will be a rather poor starting point for many floppy molecules, and their determination nontrivial for systems with thousands of atoms. Furthermore, it should be noted that normal coordinates, by construction, are nonlocal. True linear scaling, as observed when duplicating PAH7, may thus not be easily obtained in general using normal coordinates. The use of more local coordinates in combination with the present scheme is certainly a very attractive perspective for future research. One line of research here could be the use of internal coordinates, though complicated due to the cumbersome form

of the kinetic energy operators. Another interesting perspective is the localization of normal coordinates, as suggested recently by Jacob and Reiher.³⁴

The predicted importance coupling approach attempts to predict mode couplings which are not strongly coupled and neglect the suggested weakly coupled ones accordingly using only the form of the normal coordinates. This approach, however appealing, was found not to work for the molecules used in this study.

Correlation effects may also be considered in the construction of approximate wave function going beyond the single Hartree product description of VSCF. In particular, the VCC approach has the promise of maintaining the same accuracy for large systems compared to small systems, when the same level of wave function approximation is used. Some of the tricks employed in this paper also led to improvements in the scaling of VCC. Furthermore, the new active terms VSCF implementation fulfills that it is well below an optimal VCC implementation in computational scaling, which is in fact not quite the case with the native VSCF algorithm.

Acknowledgment. This work has been supported by the Lundbeck Foundation and DCSC (Danish Center for Scientific Computing). O.C. acknowledges support from the Danish national research foundation, the Lundbeck Foundation, The Danish Natural Science Research Council (Grant No. 21-04-0268), and EUROHORCs through a EURYI award.

Supporting Information Available: Figures containing the raw data and fitted curves from which the computational scaling and prefactors are found. This material is available free of charge via the Internet at <http://pubs.acs.org>.

References

- (1) White, C. A.; Johnson, B. G.; Gill, P. M. W.; Head-Gordon, M. *Chem. Phys. Lett.* **1994**, *230*, 8.
- (2) Strain, M. C.; Scuseria, G. E.; Frisch, M. J. *Science* **1996**, *271*, 51.
- (3) Ochsenfeld, C.; Kussmann, J.; Lambrecht, D. S. In *Linear-Scaling Methods in Quantum Chemistry*; Lipkowitz, K. B., Cundari, T. R., Eds.; VCH: New York, 2007; pp 1–82.
- (4) Scuseria, G.; Ayala, P. *J. Chem. Phys.* **1999**, *111*, 8330.
- (5) Subotnik, J.; Sodt, A.; Head-Gordon, M. *J. Chem. Phys.* **2006**, *125*, 074116.
- (6) Christiansen, O.; Manninen, P.; Olsen, J.; Jørgensen, P. *J. Chem. Phys.* **2006**, *124*, 084103.
- (7) Jelski, D. A.; Haley, R. D.; Bowman, J. M. *J. Comput. Chem.* **1996**, *17*, 1645.
- (8) Makri, N. *Annu. Rev. Phys. Chem.* **1999**, *50*, 167.
- (9) Roitberg, A.; Gerber, R. B.; Elber, R.; Ratner, M. A. *Science* **1995**, *268*, 1319.
- (10) Bowman, J. M. *Acc. Chem. Res.* **1986**, *19*, 202.
- (11) Gerber, R. B.; Ratner, M. A. *Adv. Chem. Phys.* **1988**, *70*, 97.
- (12) Seidler, P.; Hansen, M. B.; Christiansen, O. *J. Chem. Phys.* **2008**, *128*, 154113.

- (13) Christiansen, O. *J. Chem. Phys.* **2004**, *120*, 2140.
- (14) Sparta, M.; Toffoli, D.; Christiansen, O. *Theor. Chem. Acc.* **2009**, *123*, 413.
- (15) Hansen, M. B.; Christiansen, O.; Toffoli, D.; Kongsted, J. *J. Chem. Phys.* **2008**, *128*, 174106.
- (16) Watson, J. K. G. *Mol. Phys.* **1968**, *15*, 479.
- (17) Toffoli, D.; Kongsted, J.; Christiansen, O. *J. Chem. Phys.* **2007**, *127*, 204106.
- (18) Jung, J. O.; Gerber, R. B. *J. Chem. Phys.* **1996**, *105*, 10332.
- (19) Carter, S.; Culik, S. J.; Bowman, J. M. *J. Chem. Phys.* **1997**, *107*, 10458.
- (20) Carter, S.; Bowman, J. M.; Harding, L. B. *Spectrochim. Acta, Part A* **1997**, *53*, 1179.
- (21) Rauhut, G. *J. Chem. Phys.* **2004**, *121*, 9313.
- (22) Pele, L.; Gerber, R. B. *J. Chem. Phys.* **2008**, *128*, 165105.
- (23) Benoit, D. M. *J. Chem. Phys.* **2004**, *120*, 562–573.
- (24) Beck, M. H.; Jäckle, A.; Worth, G. A.; Meyer, H.-D. *Phys. Rev.* **2000**, *324*, 1.
- (25) Yagi, K.; Taketsugu, T.; Hirao, K.; Gordon, M. S. *J. Chem. Phys.* **2000**, *113*, 1005.
- (26) Benoit, D. *J. Chem. Phys.* **2006**, *125*, 244110.
- (27) Sparta, M.; Høyvik, I. M.; Toffoli, D.; Christiansen, O. *J. Phys. Chem. A* **2009**, *113*, 8712.
- (28) MidasCpp (Molecular Interactions, Dynamics and Simulation Chemistry Program Package in C++), <http://www.chem.au.dk/~midas>, accessed Nov. 8, 2009.
- (29) Stewart, J. J. P. *J. Comput. Chem.* **1989**, *10*, 209.
- (30) Stewart, J. J. P. *J. Comput. Chem.* **1989**, *10*, 221.
- (31) Schmidt, M. W.; Baldridge, K. K.; Boatz, J. A.; Elbert, S. T.; Gordon, M. S.; Jensen, J. H.; Koseki, S.; Matsunaga, N.; Nguyen, K. A.; Su, S.; Windus, T. L.; Dupuis, M.; Montgomery, J. A. *J. Comput. Chem.* **1993**, *14*, 1347.
- (32) Gordon, M. S.; Schmidt, M. W. In *Advances in Electronic Structure Theory: GAMESS a Decade Later*; Dykstra, C. E., Frenking, G., Kim, K. S., Scuseria, G. E., Eds.; Elsevier: Amsterdam, 2005; pp 1167–1190.
- (33) Christiansen, O. *J. Chem. Phys.* **2004**, *120*, 2149.
- (34) Jacob, C. R.; Reiher, M. *J. Chem. Phys.* **2009**, *130*, 084106.

CT9004454